Smart Structures and Systems, *Vol. 12, No. 6 (2013) 679-694*
DOI:http://dx.doi.org/10.12989/sss.2013.12.6.679

Vibration based damage localization using MEMS on a suspension bridge model

Marco Domaneschi[*1], Maria Pina Limongelli[2] and Luca Martinelli[1]

[1]*DICA, Politecnico di Milano, Milano Italy*
[2]*ABC, Politecnico di Milano, Milano Italy*

(Received July 5, 2012, Revised June 29, 2013, Accepted July 16, 2013)

Abstract. In this paper the application of the Interpolation Damage Detection Method to the numerical model of a suspension bridge instrumented with a network of Micro-Electro-Mechanical System sensors is presented. The method, which, in its present formulation, belongs to Level II damage identification method, can identify the presence and the location of damage from responses recorded on the structure before and after a seismic damaging event. The application of the method does not require knowledge of the modal properties of the structure nor a numerical model of it. Emphasis is placed herein on the influence of recorded signals noise on the reliability of the results given by the Interpolation Damage Detection Method. The response of a suspension bridge to seismic excitation is computed from a numerical model and artificially corrupted with random noise characteristic of two families of Micro-Electro-Mechanical System accelerometers. The reliability of the results is checked for different damage scenarios.

Keywords: damage localization; IDDM; MEMS; noise; suspension bridge; earthquake

1. Introduction

Structural health monitoring of long span bridges using vibration techniques received an increasing attention in the last two decades as an efficient alternative to other techniques, such as visual inspection.

Changes of modal properties of the structure, that can be identified from vibration responses, have been proposed and widely used in literature as damage detecting feature and successfully applied to detect and localize damage in different types of structures (Doebling *et al.* 1996, Sohn *et al.* 2003). One of the drawbacks related to the use of modal parameters as damage detecting features is related to their sensitivity to environmental changes such as temperature or operational conditions that somehow hinders robust and reliable estimations.

For large structures such as long span bridges this influence can be of particular importance due to the extension of the structure. Furthermore, the estimation of modal parameters requires the application of identification procedures that are not always feasible to be used in automatic monitoring systems, a category that have become more and more important for maintenance of strategic structures such as long span bridges.

∗Corresponding author, Ph.D., E-mail: marco.domaneschi@polimi.it

http://www.techno-press.org/?journal=sss&subpage=8 ISSN: 1738-1584 (Print), 1738-1991 (Online)

Some of the shortcomings related to the use of modal properties can be alleviated by using methods based on the analysis of spatial data, namely the operational deformed shapes of the structure, that use damage detecting features that can be directly recovered from recorded data thus speeding the process of damage detection and allowing, if required, to setup an automated monitoring system.

In (Casciati *et al.* 2005a,b) a statistical method based on the response surface approximation theory (De Grandis *et al.* 2009) to approximate the relationship between the measurements collected by different FOS (fibre optic sensors) during the same test is applied to the collected data to detect and locate the damages of different intensities. In the Gapped Smoothing Method (GSM) proposed by (Ratcliffe 2000), damage is indicated as a deviation of the displacement curvature from a smooth and continuous cubic polynomial model.

In the Frequency Response Curvature Method (FRCM) proposed by (Sampaio *et al.* 1999) the damage index is defined in terms of variations of the displacement curvature calculated from frequency response functions (FRFs) in the inspection phase with respect to a reference state. The displacement curvature points out quick changes of rotations in the displacement profile due to a reduction of stiffness hence this feature is directly related to damage in terms of stiffness loss. On the other hand the double differentiation required to estimate this parameter introduces a loss of accuracy in the damage detecting process due to the numerical errors that are particularly high in case of real noisy signals.

The Interpolation Damage Detection Method, recently proposed and applied to several types of structures (Limongelli 2010, 2011), tries to overcome this drawback by defining the damage detecting feature in terms of displacements instead of curvatures hence reducing errors connected with differentiation. Nonetheless the reliability and robustness of the Interpolation Damage Detection Method (IDDM) still exhibits sensitivity to the level of noise in recorded signals.

Hence one of the most challenging aspects of this family of methods lies in the influence of noise in recorded responses that in some cases masks the existence and the location of damage. Therefore, to assess the robustness of the proposed techniques for damage localization, several authors perform parametric studies of the identification errors with respect to clean and noise-corrupted data (e.g., Ciambella *et al.* 2001).

To this respect the accuracy and sensitivity of recording sensors plays a significant role since sensor’s noise has the deleterious result of degrading the output of the sensor affecting the quality of the information the sensors provide and shielding or distorting the picture of the physical phenomena it should produce.

A correct choice of the type and characteristics of the sensors deployed on the structure is thus of paramount importance for the entire health monitoring process.

In the last twenty years a large research effort has been made on the use of MEMS (Micro-Electro-Mechanical System) sensors, and particularly micro-accelerometers, for dynamic health monitoring of civil structures. Among the several types of sensing schemes for micro-accelerometers, piezo-resistive, resonant, tunneling-current and capacitive, these latter have become more attractive for health monitoring purposes due to their high sensitivity, low noise, low temperature sensitivity and low power dissipation that makes them also feasible for wireless monitoring applications.

Commercial MEMS sensors range from very cheap devices, with a cost of few euros per channel, developed for cellular phones applications or automotive ones, to sensors specifically developed for seismological applications with a cost per channel in the order of 10^2 euros.

The increase of cost corresponds to a reduction of the sensor noise, hence increases the possibility to reliably detect damage through an effective damage detection method based on data recorded by the sensors deployed on the structure.

In this paper the sensitivity to noise of the IDDM is investigated with reference to the case of a seismically excited long span suspension bridge instrumented with MEMS capacitive sensors. Results obtained by considering MEMS sensors belonging to two different classes, economic and best-in class, having vastly different cost-per-channel, are compared using the responses calculated for a numerical model of a long-span bridge, namely the Shimotsui–Seto bridge (JP), subjected to seismic excitation.

Several damage scenarios, characterized by different location and severity of damage, have been modeled by a localized reduction of the bridge deck stiffness.

Results clearly show that the method does not give correct information neither about location, nor about the existence of damage, if the more economical sensors are used. On the contrary, the use of the low noise, more expensive, MEMS sensors, allows to correctly localize damage, whatever its location and severity.

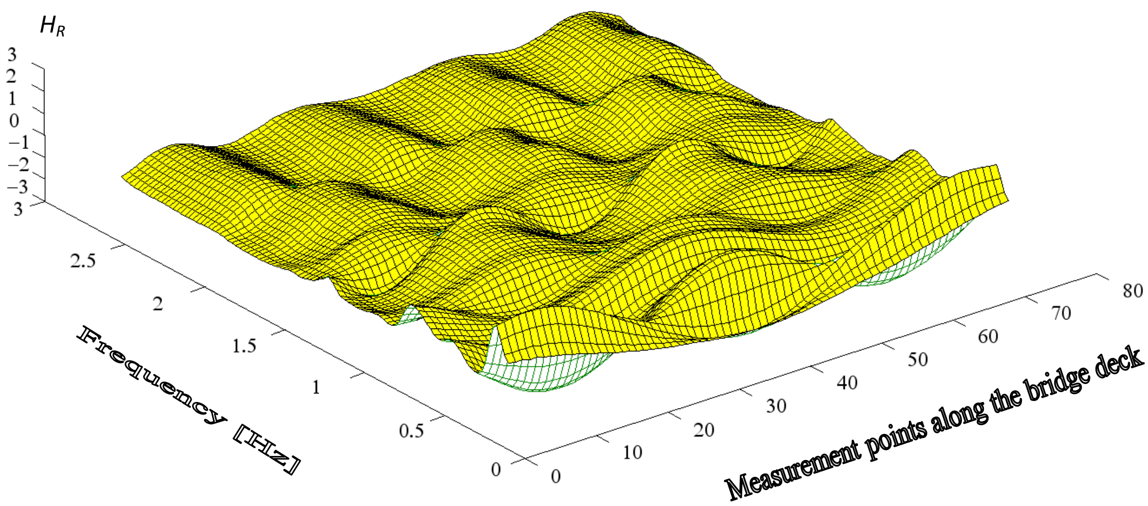

Fig. 1 Transfer functions $H_R(z_l,f)$ for lateral displacements for stations from 1 to 71 and for frequencies from 0 to 2.5 Hz

2. IDDM damage localization procedure

In the Interpolation Damage Detection Method the damage detecting feature is defined in terms of the error related to the use of a spline function in modeling the deformation profile of the bridge. Specifically, at a given location the modeling accuracy is defined as the difference between the displacement actually measured and the displacement computed at that same location by interpolating the displacements measured at all the other locations. The possible increase of the interpolation error at one instrumented location between a reference (undamaged) state and the inspection state (possibly, a damaged state) is an indication of the existence of damage close to the location where the change is detected.

In case the input excitation of the structure is known, the displacement profile, both in the reference and in the inspection phase, can be defined in terms of the transfer function (TF) of the absolute acceleration. For the case of seismic excitation the TF at each location is calculated with respect to the known base excitation. The transfer functions between the acceleration at the base and the absolute acceleration of the measurement points provide the "Operational Deformed Shape" (ODS) at that frequency. In Fig. 1 a surface representation of such functions is reported for the numerical model of the bridge that will be addresses in section 4, for the frequency range 0.2÷2.5 Hz, assuming that responses are recorded at 71 locations along the bridge deck.

At the *l*-th location z_l, the spline interpolation error is defined as the difference of the transfer function H_R, calculated from the recorded signals, and the function H_S calculated through interpolation of the transfer functions H_R at all the other instrumented locations.

Namely at each frequency f_i, the interpolated transfer function H_S (z_l, f_i) at the *l*-th location z_l is computed by spline interpolation of the transfer functions H_R (z_k, f_i) calculated from signals recorded at all the other locations (z_k, $k \neq l$).

$$H_S(z_l, f_i) = \sum_{j=0}^{3} c_{j,l}(f_i)(z_l - z_{l-1})^j \tag{1}$$

Where the coefficients (c_{0l}, c_{1l} c_{2l} c_{3l}) are functions of the $H_R(z_k, f_i)$ at locations (z_k, $k \neq l$)

$$c_{j,l}(f_i) = g(H_R(z_k, f_i)) \qquad\qquad k \neq l \tag{2}$$

The interpolation error at location z_l at the *i*-th frequency value f_i, is defined as the difference between the magnitudes of recorded and interpolated transfer functions

$$\Delta H(z_l, f_i) = |H_R(z_l, f_i) - H_S(z_l, f_i)| \tag{3}$$

Where H_R is the transfer function of the response recorded at location z_l and H_S is the spline interpolation at z_l. In order to characterize each location with a single error parameter, the norm of the error on the significant range of frequencies has been considered

$$E(z_l) = \sum_{i=N_o}^{N_o+N} \sqrt{\Delta H^2(z_l, f_i)} \tag{4}$$

N_o is the first frequency line and N is the number of frequency lines corresponding to the frequency interval where the signal to noise ratio is sufficiently large to allow for a correct definition of the transfer function.

The interpolation error at each location is computed from the difference between the actual transfer function and a spline interpolated transfer function. The difference is cumulated over the entire range of frequencies in which the signal to noise ratio is significant. The quality of measured Frequency Response Functions is adversely affected by unavoidable noise sources such as test environment, non-linear effects and noise in electronic devices. These effects are particularly important in frequency ranges where the amplitude of the response is low, such as the ones far from resonance, or those corresponding to low energy content in the input signal. In order to remove these effects, the frequency range considered in the evaluation of the interpolation error and defined by N_0 and N in Eq. (4), is chosen as to include all and only the modes that contribute to the response that is the ones that clearly appear as peaks in the magnitude of the measured frequency response function. This criterion allows considering the full dynamic of the bridge and also to filter out from the response frequency ranges where the signal to noise ratio is very low.

The values of the transfer function depends on the state of the structure, hence if the estimation of the error function through Eq. (4) is repeated in the baseline (undamaged) and in the inspection (potentially damaged) phases, the comparison between the two values, respectively E_0 and E_d gives an indication about the existence of damage at the considered location.

$$\Delta E(z_l) = E_d(z_l) - E_o(z_l) \tag{5}$$

An increase of the interpolation error between a reference and the current configuration, points out a variation of the operational deformed shape hence a variation of stiffness associated with damage close to location z_l.

In order to remove the effect of random variations of ΔE and assuming a Normal distribution of this function, the 98% percentile is assumed as a minimum value beyond which no damage is considered at that location. In other words, a given location is considered close to a damaged portion of the structure if the variation of the interpolation error exceeds the threshold calculated in terms of the mean $\mu_{\Delta E}$ and variance e $\sigma_{\Delta E}$ of the damage parameter ΔE on the population of available values (that is calculated at all the instrumented locations z_1 to z_n)

$$\Delta E(z_l) > \mu_{\Delta E} + 2\sigma_{\Delta E} \tag{6}$$

The damage index is then defined by the relation:

$$D(z_l) = \Delta E(z_l) - (\mu_{\Delta E} + 2\sigma_{\Delta E}) \geq 0 \tag{7}$$

The need to define a minimum value for the damage indicator arises since this response parameter can take non-zero values also at locations far from the damaged portions of the structure, in addition to those actually close to the damaged zone. Such circumstance would lead to a number of "false alarms", i.e. sections erroneously considered damaged, if the definition of the damage parameter would not consider the random nature of ΔE. This is carried out by defining a threshold value at a given fractile of the probability distribution of the damage parameter.

A reduction of the fractile value, to which an increase of the threshold value of the damage index $D(z_l)$ would be associated, would lead to a reduction of the false alarm risk but, at the same time, to an increased risk of "missed" alarms related to the possibility that also in the section actually damaged, the damage index does not exceed the threshold value. The choice of the minimum value of the damage index has to be the subject of a preliminary analysis, carried out on the structure so as to permit its determination on the basis of an acceptable compromise between the risk of having "false alarms" and of having "missed alarms".

Besides these observations, some logical and physical considerations on the value of the threshold suggest that a damage detecting algorithm is “efficient” if an upper bound of the threshold is defined through robustness considerations (Frangopol *et al.* 2011, Starossek and Hamberland 2011) as the value corresponding to the serviceability damage level, for example in terms of loss of stiffness with respect to the undamaged state. This requires of course the knowledge of the relationship between the value of the damage index and the loss of stiffness. This task is currently being studied for the IDDM method and will be the object of future investigations.

The main advantage of the IDDM with respect to other methods of damage localization is that it does not require a numerical model of the structure as well as an intense data post-processing or user interaction. For these reasons this method appears as a valid option for automated damage assessment, able to provide after a damaging event, reliable information about the location of damage.

As for the majority of damage detection methods, the capability of the IDDM to locate damage is influenced by the level of noise: in order to detect small reductions of stiffness, high quality signals must be recorded on the structure.

In this paper the focus is on the comparison between results that can be obtained through the application of the IDDM using sensors of different quality corresponding to different level of noise in recorded signals.

3. Modeling of noise in MEMS accelerometers

The MEMS acronym stands for “Micro Electro-Mechanical Systems”, indicating electromechanical devices with moving mechanical parts with dimensions in the range from one-millionth of a meter to a millimeter. The manufacturing processes derive from those adopted for the production of electronic circuits in silicon, allowing to couple in a small space both the “mechanical" part of the sensor as well as the control electronics, leading to sensors of smaller size and cost, with respect to similar sensors obtained with traditional technology.

The same features that allowed MEMS to become pervasive and wide-spread (i.e., the presence of both a micro-mechanical and electronic part in a single chip) give rise to the peculiar types and sources of noise in these sensors. Noise in MEMS is more important than for sensors based on classical technology, due to the small mass of the mechanical sensing part that can be easily excited by the noise energy.

Noise in MEMS can be classified, according to its origin, in external (extrinsic) and internal (intrinsic). Several intrinsic sources of noise can be present at the same time depending on the specific micromechanical mechanism (cantilevers, beams, membranes, inter-digitated electrodes, etc.) and electronics (capacitive, piezoelectric, piezoresistive, tunneling) of the MEMS accelerometric sensor. The interested reader is referred to the excellent reference (Mohd-Yasin *et al.* 2010) for a recent overview of these widely different noise sources in MEMS.

The consequence of noise presence are larger when the measured signal is weaker, since larger can be the distortion in the signal representation. In MEMS accelerometers the noise characteristics limit the smaller acceleration that can be reliably measured, thus establishing the limits in the performance of the sensor.

Attention is focused herein on capacitive MEMS accelerometers due to their superior performance at low frequencies. Typical noise sources in capacitive MEMS accelerometers have been identified in the mechanical, thermal-mechanical noise, Flicker noise, Shot noise.

Noise varies with frequency in capacitive MEMS accelerometers. It has to be pointed out that each MEM sensor has its specific noise characteristics that depend of the peculiar sensing principle, dimension, materials, and electronic implementations. This complicated noise scenario can however be simplified for structural applications since the bandwidth of interest for the structural response is normally limited (the structure can be treated as a narrow banded system) with respect to the bandwidth associated to large variation of the noise level. The expected variations with frequencies of the noise level are thus small and can be considered constant over the measurement bandwidth. This allows modeling the noise level assuming a constant value of the power spectral density over the measurement bandwidth. Measurement noises are assumed to be identically distributed, statistically independent Gaussian white noise processes (Ohtori *et al.* 2004, Dyke *et al.* 2003, Caicedo *et al.* 2003) with power spectral density function

The RMS value of noise can thus be modeled as:

$$I_{noise} = \nu\sqrt{B} \tag{8}$$

Being B the measurement bandwidth and ν the μg/√Hz noise characteristic of the employed MEM sensor reported by fabricator of MEMS sensors in their chip data-sheet.

4. Application to the suspension bridge

The suspension bridge herein considered as object of the damage detection application is the Shimotsui-Seto bridge (Fig. 2), located in Japan . It spans from the side of Mt. Washu to the Hitsuishijima Island and has a single span stiffened truss steel main girder.

The main geometric dimensions of this structure are a length of 1400 m, a main central span of 940 m, towers of height 149 m, a vertical distance of 31 m for the main girder from the extrados of towers foundations, a main girder of section 30x13 m, width and thickness respectively (Domaneschi and Martinelli 2013).

Fig. 2 Shimotsui-Seto suspension bridge (by Tatushin, September, 2008; with permission)

4.1 Numerical model

A numerical model of the Shimotsui-Seto bridge has been implemented in the ANSYS finite element code, basing on design drawings, and calibrated using the values of measured periods for the first natural modes of vibration. The model has been used as framework to perform transient seismic analyses aimed to check the performance of the damage detection procedure described in the previous sections in association to sensors noise.

Two numerical models were developed at different refinement levels. At first, a detailed model (*Model D*) implementing almost a one to one correspondence between structural and FE elements was developed. A second simplified model (*Model S*) was defined in order to reduce the computation efforts, as it is customary in case of preliminary or repeated analyses. In *Model S* the bridge deck was simulated by an equivalent Timoshenko beam able to reproduce the dynamic characteristic of the bridge in terms of frequency and mode shapes, as confirmed by the resulting MAC index close to 0.99, for the first four modes (Allemang and Brown 1982).

Two types of elements have been used in both the *D* and *S Model* (Figs. 3(a) and 3(b) respectively): beams for the towers and the deck; tension-only trusses for the main cables and the hangers.

The geometric characteristics of the beam elements have been fixed basing on the real dimensions of the structural members while the mechanical parameters have been estimated basing on the comparison between the values of the first modal periods and shapes calculated on the numerical model with those measured on the real structure. Namely for the Poisson modulus a value μ = 0.3 has been assumed for all elements; the elastic modulus of steel has been assumed equal to E = 210000000 KN/m^2 for the deck and equal to E = 165000000 KN/m^2 for the hangers; a mass density of γ = 78 $KNm^{-3}g^{-1}$ and γ = 70 $KNm^{-3}g^{-1}$ has been assumed for respectively the deck and the hangers. Both models are fully restrained to the ground at the towers' foundations and at the ends of the main cables. At the bents, dynamic translations and twist rotation are restrained while the remaining flexural rotations of the main girder are free. The deck is also fixed to the towers for transversal, vertical and twist movements. The *S Model* only has been used for the repeated transient analyses under seismic input. The interested reader is pointed to (Domaneschi and Martinelli 2013) for further details on the *D* and *S* numerical models.

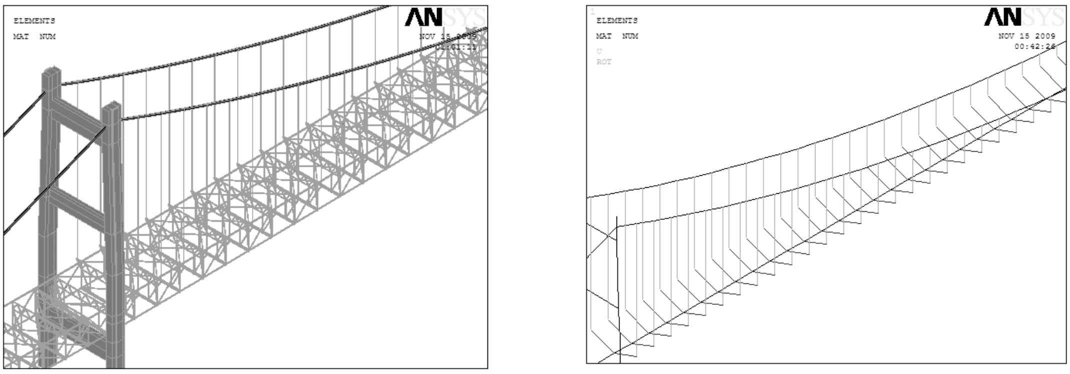

(a) (b)

Fig. 3 (a) Detailed bridge model with a one-to-one member to F.E. correspondence and (b) simplified bridge model for time-histories numerical analyses

4.2 Sensors position and noise level

The bridge has been assumed to be instrumented with a network of unidirectional MEM accelerometric sensors located on the deck at each node of the finite element model, recording transversal horizontal accelerations. The nodes of the central span of the deck, see Fig. 4, are numbered from N1 to N71 with node N36 at the deck mid-span. This number of sensors can seem large, the cost however can be almost zeroed if low-cost sensors, as it is the case for some MEM

sensors, are selected. By converse, while it is well known that MEM accelerometric sensors can be very economic, it is also known that economic MEM sensors have higher levels of sensor noise. It becomes then interesting to evaluate the level of sensors' noise to positively identify and locate damage presence. To this end, a network of MEM sensors has been assumed to be deployed on the bridge deck and, in order to simulate the measurement noise of the sensors, responses of the numerical model have been corrupted with a white noise modeled as described in Section 3. Two different families of MEM sensors have been compared herein, having vastly different cost-per-channel.
The first family is representative of sensors (denoted as *HN* "High Noise" in the following) with a cost in the order of few euro per channel, developed for cellular phones applications or automotive one, statistically mass calibrated at the factory. The second family is representative of MEM sensors of a higher class (denoted as *LN* "Low Noise" in the following), specifically developed for seismological applications and a cost per channel in the order of 10^2 euro.

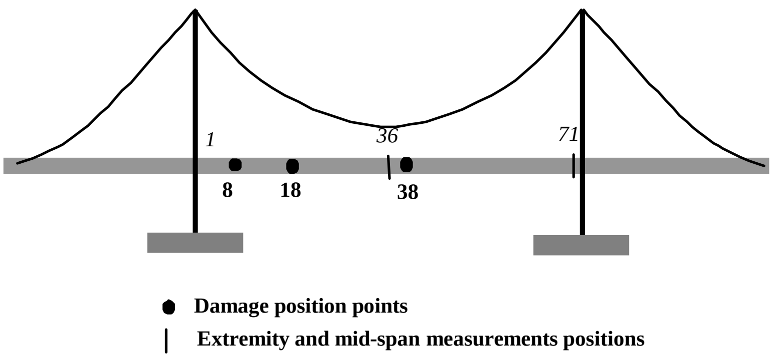

Fig. 4 Location of acceleration measurements points

To the "Low Noise" family it has been assigned a noise characteristic of 30 g/√Hz, representative of an average noise values for capacitive sensors with a measuring range of ±2 *g*, e.g. (Chae *et al.* 2004). These sensors were the state of the art around 2000 and are now in mass production. The second, "High Noise" family, is representative of MEM sensors of a higher class, with a noise characteristic of 500g/√Hz. These have been more recently developed and represented the fore-front for mass production at 2005 (Chae *et al*. 2004, Martinelli 2008).

For both sensors a 100Hz measurement bandwidth has been assumed, equal to the Nyquist frequency of the signals, being 200 Hz the sampling frequency of the simulated response of the numerical models.

4.3 Damage scenarios and earthquake loading

Several damage scenarios have been considered in order to test the sensitivity of the method to the position of the damage and the noise level. In each scenario damage was simulated by a reduction of the elastic modulus of two beam elements joined at one of the measurement points along the bridge deck.

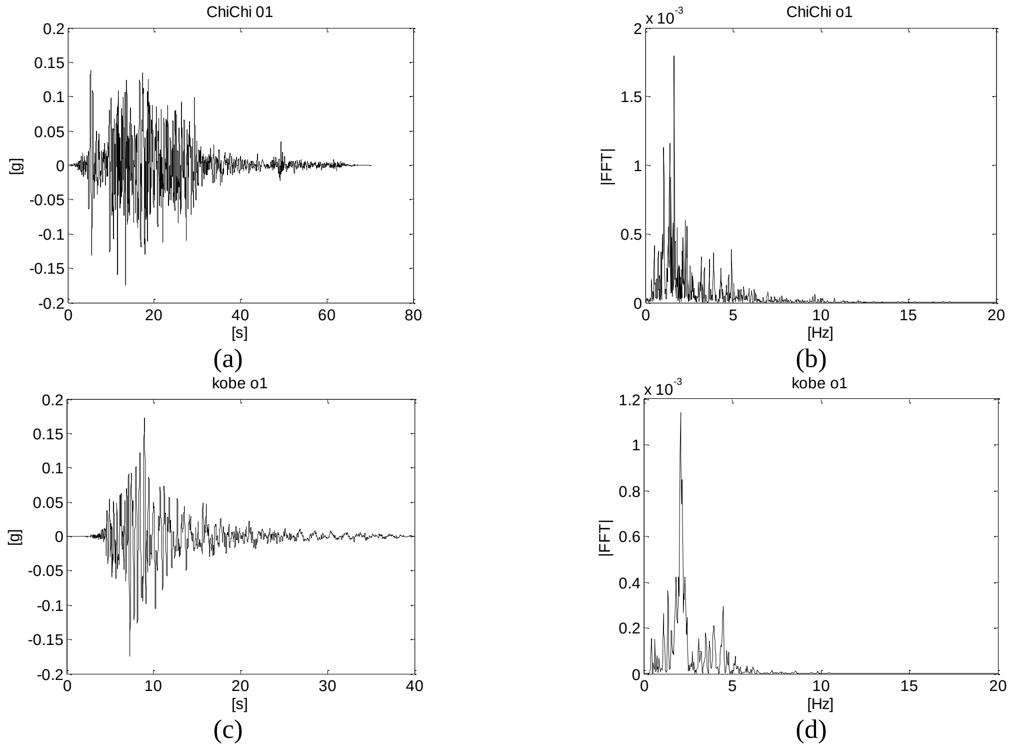

Fig. 5 Earthquake loading in the bridge longitudinal direction: ChiChi time domain (a) and frequency domain (b), Kobe time domain (c) and frequency domain (d)

A reduction of 30% to 50% of the elastic modulus has been considered, consistently with the values simulated in previous works of literature (Koh and Dyke 2007, Ntotsios *et al.* 2009, Casciati *et al.* 2004, Casciati *et al.* 2005a,b). The denomination of each damage scenario indicates the number of the node where the two damaged beams join and the amount of stiffness reduction: N18_30% means a 30% reduction of the elastic modulus of the two beams joined at node 18 of the numerical model.

The following six damage scenarios were investigated:

a) damage at the two beams joined at node N8 (30% and 50% stiffness reduction);
b) damage at the two beams joined at node N18 (30% and 50% stiffness reduction),
c) damage at the two beams joined at node N38 (30% and 50% stiffness reduction).

Earthquake loading is applied at the support point of the bridge (base of towers and bents) in the form of synchronous fully 3-Dimensional acceleration time histories of natural events. The signal recorded during the Chi-Chi, Taiwan on 1999/09/20 at station TCU072 (source CWB) was used as input in the undamaged configuration of the bridge.

The damaged structure was tested with the signal recorded in Kobe on 01/16/1995 at station Nishi-Akashi (source CUE). The choice of considering different excitation sources for identifying the structural undamaged and damaged signatures aims to reproduce the real conditions where the proposed procedure could perform.

Both records were scaled to a PGA of 0.175*g* in order to simulate the acquisition of information from earthquakes representative of after-shock seismic motions, not likely to induce (additional) damage to the structure. Fig. 5 depicts the time histories of the transversal horizontal component in time and frequency domain of the input accelerations.

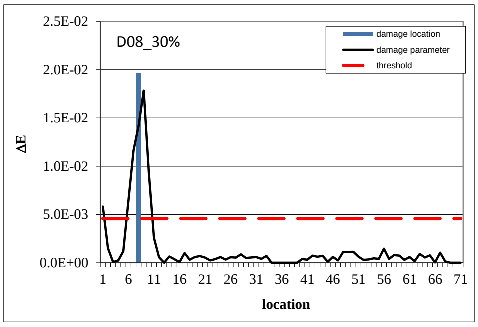

(a)

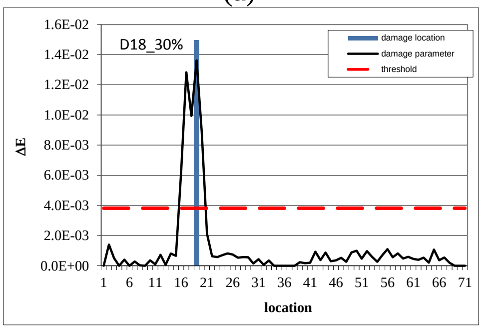

(b)

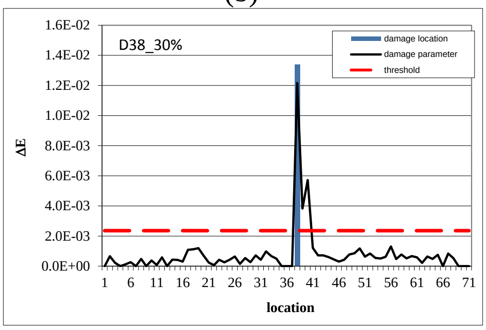

(c)

Fig. 6 Results for the IDDM method without noise for damage simulated through a 30% stiffness reduction at (a) node N8, (b) node 18 and (c) node 38

5. Damage localization

Results given by the IDDM procedure for the condition without noise corruption and the ones considering the two families (HN and LN) of sensors are reported in Figs. 6-8 respectively, where subfigures (a) are related to node N8, (b) to node N18, (c) to Node N38. A comparison is shown in terms of the values of the damage parameter ΔE defined by Eq. (5) and the 2% fractile ($\mu_{\Delta E} + 2\sigma_{\Delta E}$) of the probability distribution of ΔE, which is the minimum value of the damage parameter in order to flag the corresponding node as close to a damaged portion of the structure. The blue vertical bar shows the actual location of damage.

All the computations of ΔE are carried out in the frequency range between 0.2*Hz* and 3.5*Hz* to mitigate numerical inaccuracies.

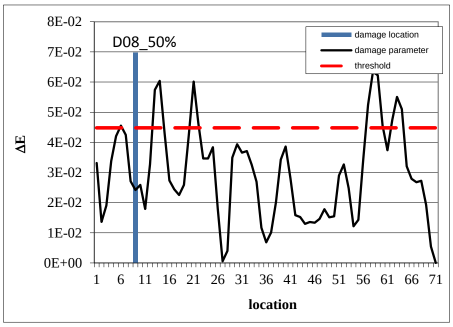

(a)

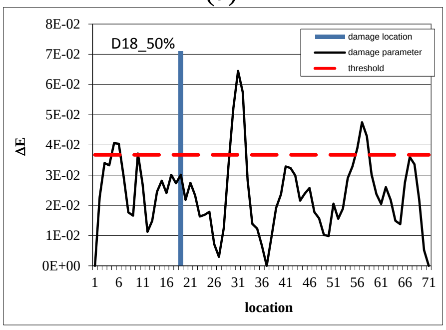

(b)

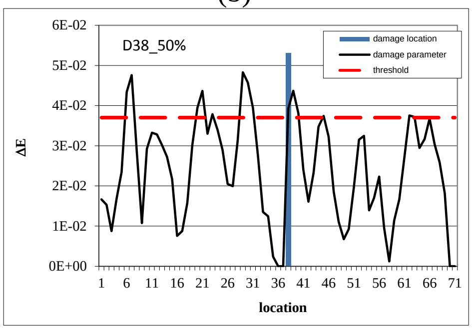

(c)

Fig. 7 Results for the IDDM method with sensors of type HN for damage simulated through 50% stiffness reduction at (a) node N8, (b) node N18 and (c) node N38

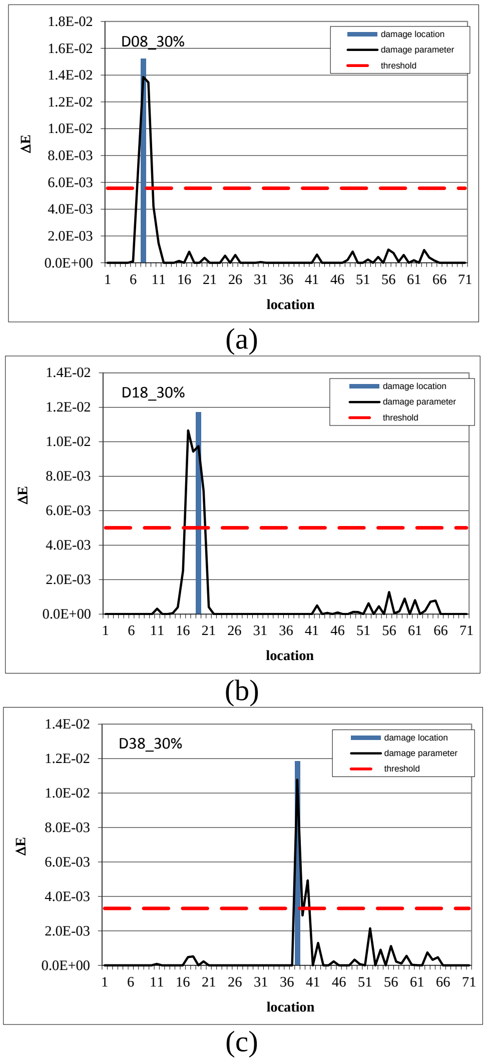

Fig. 8 Results for the IDDM method with sensors of type LN for damage simulated through a 30% stiffness reduction at (a) node N8, (b) node N18 and (c) node N38

Figs. 6(a)-6(c) depict the results obtained by applying the IDDM using responses not affected by noise in order to point out the influence of noise on results. The damage is always correctly identified.

Figs. 7(a)-7(c) depict results given by the IDDM for a damage severity of 50% in case the high noise (HN) type of sensors are used. Results are clearly inadequate since a positive and satisfactory damage detection and localization is never achieved. Several false alarms are given by the method and the actual location of damage is never found. The high level of noise completely masks the increase of the interpolation error due to damage thus strongly reducing the effectiveness of damage localization. Results for the 30% stiffness reduction are not shown in this case since not meaningful.

Changing the sensor type to the low noise (*LN*) one brings a vast improvement. In Figs. 8(a)-8(c) the results for a lower damage level (30%) are shown. The procedure shows good accuracy and efficiency, being able to correctly determine the location of the damage for all the considered damage scenarios. No false alarms are recorded and the actual location of damage is detected in all cases even for a lower severity of damage.

One last remark should be made on the number of recorded responses necessary to reach an acceptable result. The accuracy in the localization of the damage depends on the density of the network of sensors: the IDDM singles out the locations of the sensors closer to the damaged ones hence the denser the network of sensors the more accurate will be the damage localization.

6. Conclusions

In this work the performance of the IDDM damage identification method has been assessed in the case of a long span suspension bridges considering sensors noise. The method is applied to a numerical model of the Shimotsui-Seto bridge for the case of low intensity earthquake excitation and different scenarios of simulated damage. The effect of measurement noise is accounted for by artificially polluting the responses of the numerical model with realistic levels of Gaussian white noise.

Results show that noise induces random variations of the damage parameter and reduces the sensitivity of the method. If economic sensors, having a high level of noise, not specifically engineered for this type of applications, are adopted, the damage is not correctly detected by the IDDM method. On the contrary, if higher class MEM sensors are used to record structural responses, the IDDM method correctly provides the damage location independently of its position, even for damage of low severity, corresponding in accuracy to the free noise condition.

Taking into account that the cost of a network of MEMS sensors, even of high class one, is at most only a fraction of percent of the construction and maintenance cost of the bridge itself, deployment of such monitoring system is considered perfectly justified from an economic point of view and feasible for an effective maintenance of strategic structures like a suspension bridge. This is also due to the possibility to use the proposed method of damage localization in an automatic manner, without requiring interaction with an operator. This makes the method promising for future applications in on-line monitoring systems and particularly useful in the case of strategic structures, such as are the road infrastructures, which are expected to be self-diagnostic for performing efficiently also in post-earthquake emergencies.

Acknowledgements

This work has been partially supported by MIUR (Ministry of Education, University and Research) under the project "Dynamic response of linear and nonlinear structures: modeling, testing and identification" (PRIN 2009).

References

Acar, C. and Shkel, A.M. (2003), “Experimental evaluation and comparative analysis of commercial variable-capacitance MEMS accelerometers”, *J. Micromech. Microeng.*, **13**(5), 634-636.

Allemang, R.J. and Brown, D.L. (1982), “A correlation coefficient for modal vector analysis”, *Proceedings of the IMAC1, The International Modal Analysis Conference*, Orlando Fl, November.

Caicedo, J.M, Dike, S.J., Moon, S.J., Bergman, L., Turan, G. and Hague, S. (2003), “Phase II benchmark control problem for seismic response of cable stayed bridges”, *J. Struct. Control*, **10**(3-4), 137-168.

Casciati, F., Domaneschi, M., Inaudi, D., Figini, A., Glisic, B. and Gupta, A. (2004), “Long-gauge fiber-optic sensors: a new approach to dynamic system identification”, *Proceedings of the 3rd European Conference on Structural Control*, Vienna, Austria.

Casciati, S., Domaneschi, M. and Inaudi, D. (2005a), “Local damage detection from dynamic SOFO experimental data”, *Proceedings of the SPIE - The International Society for Optical Engineering*, **5765**, 591-599, DOI: 10.1117/12.600440.

Casciati, S., Domaneschi, M. and Inaudi, D. (2005b), “Damage assessment from SOFO dynamic measurements”, *Proceedings of the SPIE - The International Society for Optical Engineering*, **5855**, 1048-1051, DOI: 10.1117/12.623656.

Chae, J., Kulah, H. and Najafi, K. (2004), “An in-plane high sensitivity, low noise micro-g silicon microaccelerometer with CMOS readout circuitry”, *J. Microelectromech. S.*, **13**(4), 628-635.

Chu, A. (2012), *Accelerometer selection based on applications*, Endevco Technical Paper TP291 (http://www.smtnet.com/library/files/upload/TP291.pdf - last access July 3, 2012).

Ciambella, J., Vestroni, F. and Vidoli, S. (2011), “Damage observability, localization and assessment based on eigenfrequencies and eigenvectors curvatures”, *Smart Struct Syst.*, **8**(2), 191-204.

De Grandis, S., Domaneschi, M. and Perotti, F. (2009), “A numerical procedure for computing the fragility of NPP components under random seismic excitation”, *Nucl. Eng. Des*., **239**(11), 2491-2499.

Dyke, S.J., Caicedo, J.M., Turan, G., Bergman, L.A. and Hague, S. (2003), “Phase I benchmark control problem for seismic response of cable-stayed bridges”, *J. Struct. Eng. - ASCE*, **129**(7), 857-872.

Doebling, S.W., Farrar, C.R., Prime, M.B. and Shevitz, D.W. (1996), *Damage identification and health monitoring of structural and mechanical systems from changes in their vibration characteristics: a literature review*, Report LA-13070-MS, Los Alamos National Laboratory.

Domaneschi, M. and Martinelli, L. (2013), “Optimal passive and semi-active control of a wind excited suspension bridge”, *Struct. Infrastruct. E.*, **9**(3), 242-259.

Frangopol, D.M., Saydam, D. and Kim, S. (2011), “Maintenance, management, life-cycle design and performance of structures and infrastructures: a brief review”, *Struct. Infrastruct. E.*, **8**(1), 1-25.

Koh, B.H. and Dyke, S.J. (2007), “Structural health monitoring for flexible bridge structures using correlation and sensitivity of modal data”, *Comput. Struct.*, **85**(3-4), 117-130.

Limongelli, M.P. (2010), “Frequency response function interpolation for damage detection under changing environment”, *Mech. Syst. Signal Pr*., **24**(8), 2898-2913.

Limongelli, M.P. (2011), “The interpolation damage detection method for frames under seismic excitation”, *J. Sound. Vib.*, **330**(22), 5474-5489.

Martinelli L. (2008), “Sull’utilizzo di accelerometri MEMS per il rilievo di vibrazioni negli edifici” (in Italian), *Proceedings of the 3rd Workshop Problemi di vibrazioni nelle strutture civili e nelle costuzioni meccaniche*, Perugia, September.

Mohd-Yasin, F., Nagel, D.J. and Korman, C.E. (2010), “Noise in MEMS”, *Meas. Sci. Technol*., **21**(1), 1-22.

Ntotsios, E., Papadimitriou, C., Panetsos, P., Karaiskos, G., Kyriakos P. and Perdikaris, P.C. (2009), “Bridge health monitoring system based on vibration mesurements”, *J. Earthq. Eng*., **7**(2), 469-493.

Ohtori, Y., Christenson, R.E., Spencer Jr., B.F. and Dyke S.J. (2004), “Benchmark Control Problems for Seismically Excited Nonlinear Buildings”, *J. Eng. Mech. - ASCE*, **130**(4), 366-385.

Ratcliffe, C.P. (2000), “A frequency and curvature based experimental method for locating damage in structures”, *J. Vib. Acoust*., **122**(3), 324-329.

Sampaio, R.P.C., Maia, N.M.M. and Silva, J.M.M. (1999), “Damage detection using the frequency response function curvature method”, *J. Sound. Vib.*, **226**(5), 1029-1042.

Sohn, H., Farrar, C.R., Hemez, F.M., Shunk, D.D., Stinmates, D.W. and Nadler, B.R. (2003), *A review of structural health monitoring literature: 1996-2001*, *Report LA-13976-MS*, Los Alamos National

Laboratory.
Starossek, U. and Haberland, M. (2011), “Approaches to measures of structural robustness”, *Struct. Infrastruct. E.*, **7**(7-8), 625-631.

CC